High-Frequency Soft-Switching PWM DC-DC Power Converter for Low Voltage Large Current Applications

Hidekazu Muraoka*, Kenya Sakamoto**, Mutsuo Nakaoka***

* Maritime Technology Department, Hiroshima National College of Maritime Technology, Hiroshima, Japan
** Department of Ocean Electro-Mechanical Engineering, Kobe University of Mercantile Marine, Kobe, Japan.
*** The Graduate School of Engineering and Science, Yamaguchi University, Yamaguchi, Japan.

Abstract- This paper presents a novel prototype version of ZCS-PWM forward DC-DC power converter using power MOSFETs which is designed for application specific low voltage large current conversion operation. The soft-switching forward power converter with a high frequency isolated transformer link which can efficiency operate over wide load ranges under two conditions of ZCS as well as active voltage clamped switching is evaluated and discussed on the basis of the simulation and experimental results.

I. INTRODUCTION

In recent years, the soft-switching PWM DC-DC power converters using MOS-gate power semiconductor devices such as power MOSFETs, IGBTs, MCTs, IEGTs, CSTBT which can efficiently operate under the principle of zero voltage and/or zero current soft-switching have attracted special interest for efficient energy conversion power conditioners. It is more acceptable for high power applications that the active voltage clamped soft-switching PWM DC-DC forward power converter operating at zero current soft-switching scheme in order to minimize the switching power losses of power semiconductor devices and power modules and EMI/RFI noises.

In this paper, it is presented that the active voltage clamped soft-switching PWM forward power converter circuit configuration, which makes use of the parasitic parameters (leakage inductance & magnetizing inductance) of forward high frequency transformer with ferrite core. In particular, it is also discussed that the quasi-resonant soft-switching PWM forward converter using power MOSFETs which is designed for a low voltage and large current applications for solar photovoltaic generator driven boat system[1]~[3] from a practical point of view.

II. SYSTEM DESCRIPTION

Fig.1 shows a schematics diagram of the power conditioning circuit for specific-application solar energy driven-boat system. Fig.1 (a) shows the solar energy driven-boat system with DC motors. [4][5] Fig.1 (b) shows the solar energy driven-boat system using AC motors with permanent magnet.

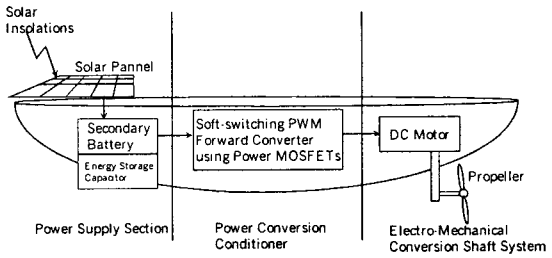

(a) Soft-switched converter drive DC motor system

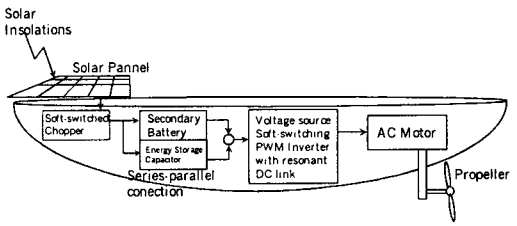

(b) Soft-switched Inverter drive AC motor system

Fig.1 Overview for two types pannel, of solar photovoltaic power-driven boat system

These power conditioning systems are composed of solar cell panel, soft-switched PWM DC-DC forward converter with a high frequency transformer link, and motor coupled direct drive mechanical propeller drive for this new energy interfaced boat system.
Table.1 indicates the design specifications of solar battery-driven DC motor coupling boat system.

Table.1 Design specifications of solar battery-driven boat system

Solar Pannel	500W, Single Crystal Type
Secondary Battery	12V, 6.5Ah×4 (2p×2s) Series resistance = 40 mΩ
Converter Output Power	1kW (MOSFET:2SK1382)
DC Motor	480W continuous

III. CONVERTER CIRCUIT IMPLEMENTATION AND ITS OPERSTION

Fig. 2 depicts the proposed forward type PWM DC-DC power converter operating at zero current soft-switching, which takes advantage of the parasitic parameters of high frequency transformer leakage and magnetizing inductance. Capacitor Ca is applied to supply reset voltage of the transformer. Ca acts as the voltage clamper instead of the resonant capacitor for soft-switching.[6]

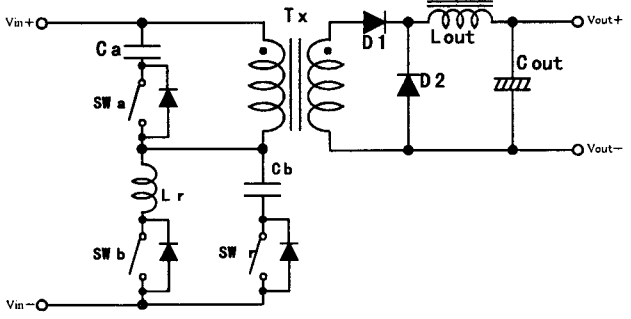

Fig.2 Soft-switching PWM forward converter using low voltage large current power MOSFETs

Delay times of switching between SWr and SWb is significant and sensitive for ZCS operation. And line inductances existing in MOSFET's (SWb) and wiring make large switching power losses for large current operation range.

Table.2 indicates the design specifications and circuit parameters of this trially-produced forward converter.

Table.3 indicates electrical characteristics of the main active switch SWb (2SK1382).

Table.2 Design specifications

Items	Symbols	Design Values
Supply Voltage	E	24 V
Active Clamped Capacitor	Ca	6.28 μ F
Quasi-Resonant Capacitor	Cb	0.9 μ F
Quasi-Resonant Inductance	Lr	0.1 μ H
Transformer	Tx	PC30EIC90(Gap:0 mm)
Primary Winding	Np	3 Turns
Secondary Winding	Ns	12 Turns
Smoothing Reactor Inductance	Lout	30 μ H
Smoothing Capacitor Capacitance	Cout	470 μ F
Main & Sub Switches	SWb、SWa	2SK1382
Resonant Switch	SWr	
Diode	D1、D2	30JL2C41
Switching Frequency	fsw	50 kHz

Table.3 Electrical characteristics of 2SK1382

Item		Symbols	Value	Unit
Drain-source voltage		VDSS	100	V
Gate-source voltage		VGSS	0	V
Drain current	DC	ID	60	A
	Pulse	IDP	240	A
Input capacitance		Ciss	8000	pF
On resistance		RDS (on)	15～20	mΩ

The zero current soft-switching is achieved by the circuit composed of four devices: quasi-resonant capacitor Cb, main switch SWb, quasi-resonant inductance Lr and resonant switch SWr. Fig.3 represent zero current soft-switching circuit.

Lr and Cb for the quasi resonance can make ZCS possible. And the quasi resonant amplitude i_r is operating under every load current condition.

$$i_r = V_{Cb}\sqrt{\frac{C_b}{L_r}}\sin\frac{1}{\sqrt{L_r C_b}}t \quad (1)$$

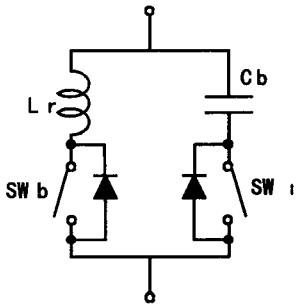

Fig.3 Zero current soft-switching circuit

Fig.4 shows the illustrative switching-time chart of SWa, SWb and SWr that give the give the switching timing frequency.

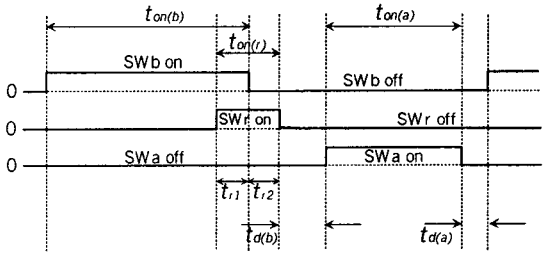

Fig.4 Switching time chart of SWa, SWb & SWr (gate-source voltage of SWa, SWb & SWr)

Delay time t_{r1} has to synchronize with the peak of the resonant current to make it zero current easier for the

main active switch SWb. The condition of each delay times is given as follows;

$$t_{r1} = \pi\sqrt{L_r C_b}/2 \tag{2}$$

$$t_{r2} > \pi\sqrt{L_r C_b}/2 \tag{3}$$

The voltage Vc_a across of active clamped capacitor influences upon $t_{on(a)}$, $t_{on(b)}$, $t_{on(r)}$ and a power supply voltage E.

$$V_{Ca} \approx -\frac{t_{on(b)} + \frac{t_{on(r)}}{2}}{t_{on(a)}} E \tag{4}$$

Fig. 5 gives the operating modes of the zero current soft-switching for forward DC-DC power converter with an active clamped capacitor.

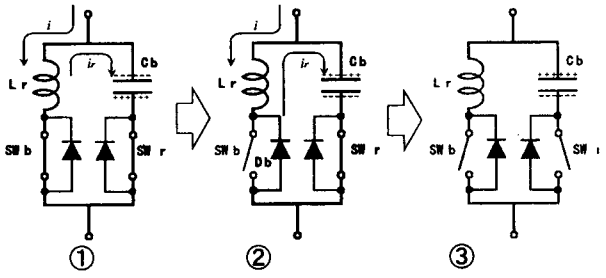

Fig.5 The operational modes transition of zero current soft-switching

This forward type ZCS-PWM DC-DC power converter has some operating modes in transient phenomena due to inductance and capacitor elements. The zero current soft-switching is achieved under those modes transition.

<mode 1>

This mode specifies a duty period flowing large current through the main active power switch SWb. The current flowing the active power switch SWb is the sum of load current and magnetizing current.

<mode 2>

After conducting the parasitic diode Db of the main active switch SWb, the active power switch SWb turns off to fall into mode 2. At this time, the active power switch SWb is under zero current condition. Therefore zero current soft-switching is achieved when the active power switch SWb turns off.

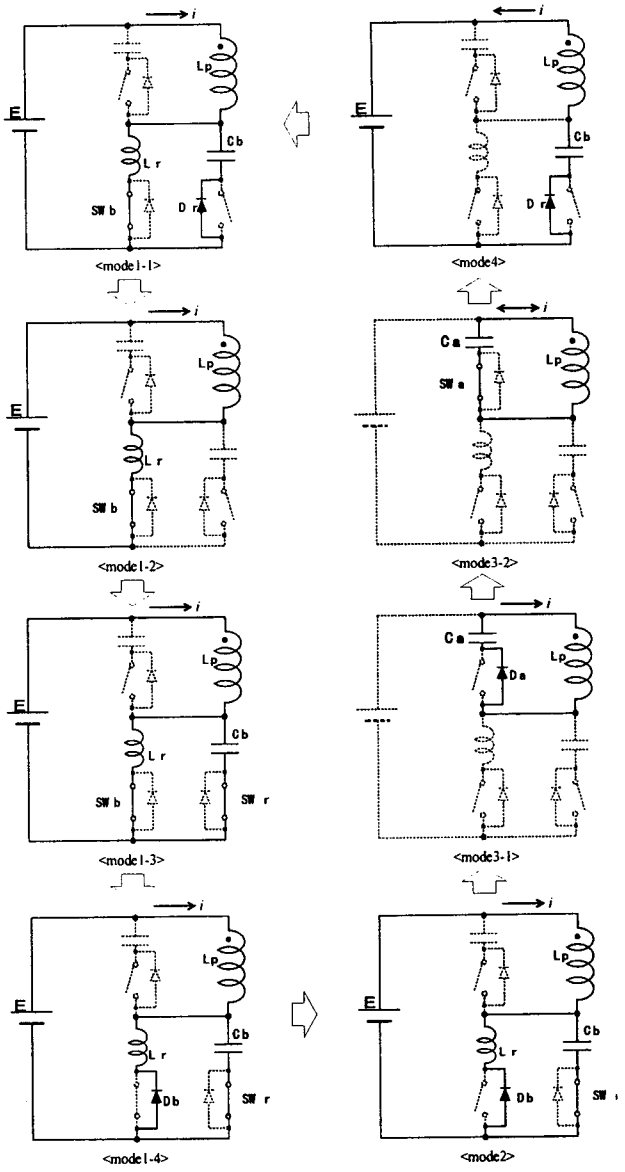

Fig.6 The operational modes of PWM forward converter operating at zero current soft-switching

<mode 3>

If the voltage across quasi-resonant capacitor Cb exceeds the voltage across active clamped capacitor Ca, the diode Da is on, and operation mode is led to mode 3_1. After the diode Da conducting, the active power switch SWa turns on that operation mode moves to mode 3_2. Therefore, ZVS-ZCS soft-switching is performed when the active power switch SWa turns on. In mode 3_2, parallel capacitors Ca and Cb are discharged after their capacitors charged by the magnetizing current.

<mode 4>

After the active power switch SWa turns off, the quasi-resonant capacitor Cb starts to discharge the voltage across loss-less capacitance of SWb.

IV. Performance Evaluations And Discussions

A. Simulation Results

Surge voltage and voltage ringing does not occur in the ideal circuit. However, the parasitic parameters exist in the actual circuit. They are concerned with in case of considering the causes of EMI noises and power losses.

Fig.7 shows the simulation circuit containing some parasitic parameters.

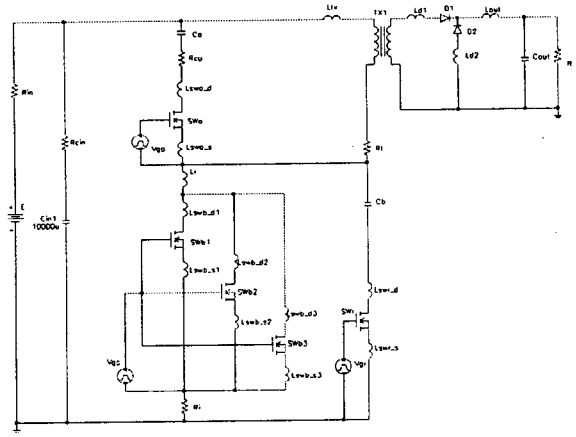

Fig.7 The simulation circuit containing parasitic parameters

Table.4 indicates the design specifications and the circuit parameters at the simulation with some parasitic parameters.

Table.4 Design specifications at the simulation with parasitic parameters.

Symbols	Design Values	Symbols	Design Values
fsw	50 kHz	*Rin*	10 mΩ
E	24 V	*Rcin*	10 mΩ
Cin	10000 μF	*Rl*	10 mΩ
Ca	6.28 μF	*Rca*	10 mΩ
Cb	0.9 μF	*Ri*	2.5 mΩ
Lr	0.1 μH	*Lsw x_x*	10 nH
Tx	(PC30EIC90) Np:3、Ns:12 Gap:0 mm	*Ltx*	0.1 μH
		Ld1	1 μH
		Ld2	10 nH
Lout	80 μH	SWb、SWa	(2SK1382)
Cout	470 μF	SWr	
R	6.5Ω	D1、D2	(30JL2C41)

Fig.8 displays the calculated drain-source voltage waveforms across SWb and drain current waveforms of SWb and SWr obtained in simulation analysis due to PSpice to perform ZCS soft-switching.

To achieve soft-switching for wide range, setting transition delay times in the switching of SWa, SWb and SWr are significant to ZCS operation.

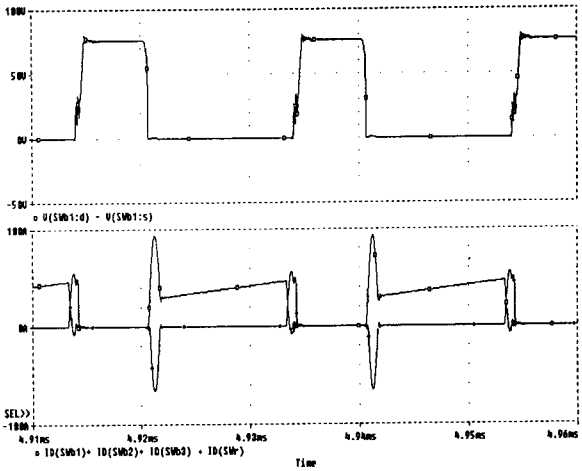

- Drain-source voltage waveforms across SWb
- Drain current waveforms of SWb and SWr

(a) ideal circuit

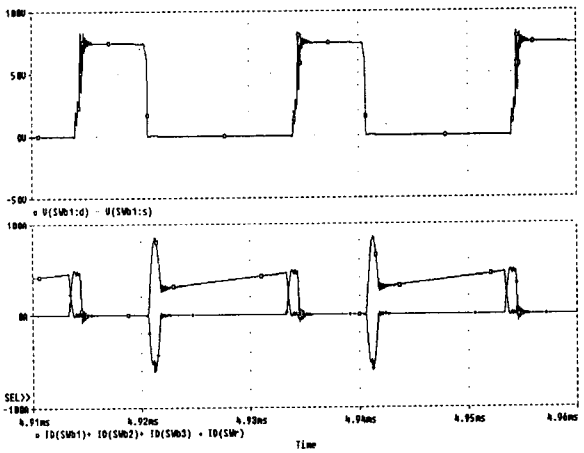

- Drain-source voltage waveforms across SWb
- Drain current waveforms of SWb and SWr

(b) actual circuit (with parasitic parameters)

Fig.8 Calculated soft-switching waveforms

(fsw=50kHz、Duty 65%、E=24V、Vout=60V、Iout=9A)

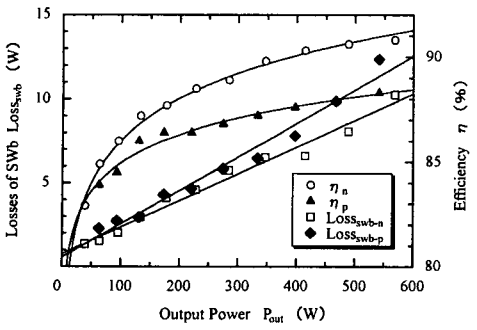

Fig.9 Calculated efficiency and switch power losses for output power
(*fsw*=50kHz、*E*=24V、*Cb*=0.9 μ F、*Lr*=0.1 μ H、t_{r1} ·t_{r2}=0.5 μ s、R=6.5 Ω)

B. Experimental Results

Fig.10 shows the measured drain-source voltage across SWb with proposed circuit. The delay times is established on the basis simulation and transient phenomena analysis : t_{r1}=0.45[μ s], t_{r2}=0.45[μ s]. Measured voltage of SWb is agreed with simulation analysis with respect to rising voltage period and around top of voltage.

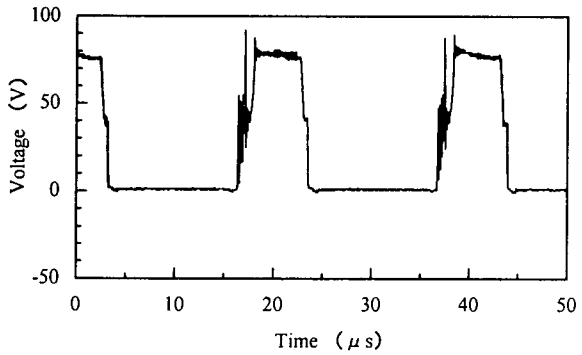

Fig.10 Measured drain-source voltage across main-switch SWb.
(fsw=50kHz、Duty 65%、E=24V、Vout=56V、Iout=8.5 A、Cb=0.9 μ F、Lr=0.1 μ H、tr1·tr2=0.45 μ s)

Fig.11 displays the measured efficiency of this forward type ZCS-PWM DC-DC power converter for output power.

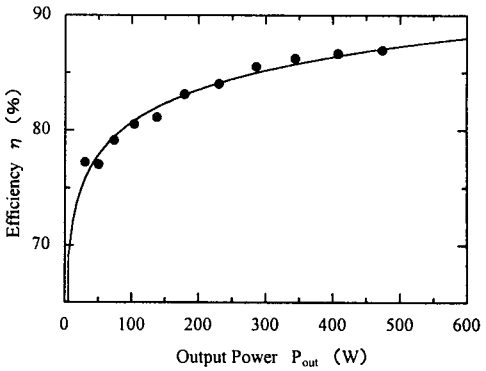

Fig.11 Measured efficiency for output power
(fsw=50kHz、E=24V、Cb=0.9 μ F、Lr=0.1 μ H、tr1 =0.6 μ s、tr2=1.05 μ s、R=6.5 Ω)

The experimental circuit can be loaded with efficiency 87.8[%] at E=24.0[V], Vout=56[V], R=6.5[Ω] and Pout=480 [W] for the present.

V. CONCLUSIONS

A specific applications power converter designed for low voltage large current solar battery generator driven boat equipment has been presented which incorporates an efficient active voltage clamped quasi-resonant PWM forward DC-DC converter operating under a principle of zero current soft-switching. Its simulation results in addition to some data of the experimental set-up have been discussed and evaluated for this power DC-DC converter. The performance of converter fed solar boat system and its effectiveness has been discussed from a practical point of view.

REFERENCES

[1] K.Sakamoto, et al., "Improvement on Efficiency of a Forward Converter with Controlled Resonant Commutation",Review of Kobe University of Mercantile Marine, part II , No.46, Jul.1998
[2] J.Kikuchi, et al, "Boosting Forward Converter", ibid. No.42, Jul.1994
[3] H. Muraoka, et al. : Soft-switching PWM forward power converter with auxiliary active clamped capacitor for solar energy-driven boat、PEDES'98 Proc. vol2 pp.683-688, Dec.1998
[4] J.Kikuchi, et al, "Dynamic Analysis of Electrical System for Solar Boat(2)", ibid. No.41, Jul.1993
[5] Solar Energy Research Group of KUMM, "Technical Report on Solar Boat 'KOYO94'", Technical Report of the International ASME Solar Boat Regatta, Jul. 1994
[6] C.P.Henze, et al, "Zero-voltage switching in high frequency power converters using pulse width modulation", IEEE APEC proc., Feb.1988